AMPK inhibits ULK1-dependent autophagosome formation and lysosomal acidification via distinct mechanisms

Running title: AMPK inhibits early and late autophagy pathways

Chinwendu Nwadike[1]*, Leon E. Williamson[1]*, Laura E. Gallagher[1], Jun-Lin Guan[2] and Edmond Y.W. Chan[1,3,4]

[1] Strathclyde Institute for Pharmacy and Biomedical Sciences. University of Strathclyde, Glasgow, Scotland G4 0RE
Tel: +44-141-548-3924

[2] Department of Cancer Biology, University of Cincinnati College of Medicine. USA

[3] Department of Biomedical and Molecular Sciences, School of Medicine, Queen's University, Canada

[4] Department of Pathology and Molecular Medicine, Kingston General Health Research Institute, Canada

Corresponding author: Edmond.Chan@Strath.ac.uk

(*) these authors contributed equally to this work

Key words:

Autophagy, amino acid starvation, glucose starvation, ULK1, MTORC1, AMPK, leucine, glutamine, arginine, lysosome acidification

Abstract

Autophagy maintains metabolism in response to starvation but each nutrient is sensed distinctly. Amino acid deficiency suppresses mechanistic target of rapamycin complex 1 (MTORC1) while glucose deficiency promotes AMP-activated protein kinase (AMPK). MTORC1 and AMPK signalling pathways converge onto the ULK1/2 autophagy initiation complex. Here, we show that amino acid starvation promoted formation of ULK1- and Sequestosome1/p62-positive early autophagosomes. Autophagosome initiation was controlled by MTORC1 sensing glutamine, leucine and arginine levels together. By contrast, glucose starvation promoted AMPK activity, phosphorylation of ULK1 Ser 555 and LC3-II accumulation, but with dynamics consistent with a block in autophagy flux. We studied the flux pathway and found that starvation of amino acid, but not of glucose, activated lysosomal acidification, which occurred independently of autophagy and ULK1. Further to lack of activation, glucose starvation inhibited the ability of amino acid starvation to activate both autophagosome formation and the lysosome. Activation of AMPK and phosphorylation of ULK1 were determined to specifically inhibit autophagosome formation. AMPK activation also was sufficient to prevent lysosome acidification. These results indicate concerted but distinct AMPK-dependent mechanisms to suppress early and late phases of autophagy.

Introduction

During macro-autophagy (herein called autophagy), cellular components are sequestered into double-bilayer membrane vesicles termed autophagosomes. Autophagosomes are transported to lysosomes followed by organellar fusion to allow content degradation and recycling of metabolic building blocks for cell viability (1, 2). A fundamental feature is that autophagy is potently induced following nutrient starvation, for example in yeast deprived of nitrogen (amino acids and ammonia)(3). Autophagy is widely appreciated as a central hub for maintaining metabolic homeostasis, which plays roles in the larger context controlling cell fate during normal ageing and cancer cell survival (4). As such, we and others have been interested in how the mammalian ULK1/2 complex coordinates multiple nutrient-dependent signals at the top of the autophagy regulatory cascade.

In one prominent model, MTORC1 phosphorylates ULK1 on Ser 757 (Ser 758 in human) which has the effect of disrupting interaction between ULK1 and AMPK (5). This direct binding allows AMPK to phosphorylate ULK1 on sites Ser317 and Ser777, which simulates ULK1 activity for autophagy. Amino acid starvation would suppress MTORC1 activity, facilitating positive autophagy regulation from AMPK. Glucose starvation would in turn activate AMPK to promote autophagy via ULK1-mediated phosphorylation of factors such as Beclin1, ATG13 and FIP200 (6, 7). This single model, however, cannot account for the full complexity of autophagy which involves other modifications on ULK1. AMPK phosphorylates ULK1 on other sites such as Ser 467, 555, 574, 637 (Ser 467, 556, 575, 638 in human), which may function for mitophagy in response to cell energy signals (8, 9). Other patterns of nutrient-sensitive phosphorylation on ULK1 have been reported and the Ser637 site appears to be controlled by both MTORC1 and AMPK, highlighting inter-connections not yet fully understood (10).

Autophagy induction following amino acid starvation is widely prevalent, robust and rapid (11-13). Autophagy following glucose starvation has also been reported but this response appears to be more complex, requiring more prolonged duration of stress to produce effects (5, 14-19). Interestingly, the MTORC1-AMPK-ULK1 interplay model predicts that autophagy following amino acid withdrawal still requires AMPK function. On this issue, the precise role of glucose starvation and AMPK in autophagy still remains controversial. Low cellular energy levels and AMPK activation were initially proposed to block autophagy based on biochemical approaches (20, 21). Other reports have shown glucose starvation to inhibit autophagy responses (22) (23, 24).

Previously, we approached this area by studying nutrient-dependent autophagy in fibroblasts derived from ULK1/2 double knockout (DKO) mice (11). We showed that ULK1/2 DKO clearly blocked the rapid autophagy response stimulated by amino acid starvation. In that work, we noted that prolonged (overnight) glucose starvation produced a distinct autophagy phenotype that was independent of canonical phosphatidylinositol 3-phosphate (PtdIns3P) signals. Here, we further investigated how amino acid and glucose starvation signals control autophagy. We find in a wide range of cells that only amino acid starvation stimulated robust bona fide autophagy degradative flux. In contrast, glucose starvation produce phenotypes resembling a reduction of flux and halted autophagy. Surprisingly, amino acid and glucose starvation showed differential control of autophagy gene expression, early autophagosome formation and activation of the lysosome. Furthermore, glucose starvation and resulting AMPK activation could over-ride and suppress amino acid starvation signals that normally trigger autophagy. These findings highlight the opposing mechanisms that allow MTOR and AMPK to balance function of both early and late stages of autophagy.

Results

Glucose starvation fails to activate autophagy flux

We have previously shown how amino acid starvation robustly activated autophagy in mouse embryonic fibroblasts (MEF) and how this response was fully blocked upon ULK1/2 DKO (11). Here, we explored alternate forms of nutrient stress. We surprisingly found that starving MEF of glucose did not strongly activate autophagy, as detected by conversion of inactive LC3-I to activated (lipid-modified) LC3-II (Fig 1A). Glucose starvation only led to relatively small increases in LC3-II that did not further accumulate when lysosomal activity was blocked by bafilomycin A1 (Baf A1), which clearly contrasted with our previous observations following amino acid starvation using the same cell system (11). Glucose starvation failed to activate Baf A1-dependent LC3-II accumulation in both short (2 hour) and prolonged (18 hour) starvation experiments. Furthermore, the mild changes in LC3-II following glucose starvation still occurred in ULK1/2 DKO MEF lines.

We confirmed that amino acid starvation within 2 hours led to clear MTORC1 suppression (S6 phosphorylation levels) and LC3 conversion (Fig 1B). Amino acid starvation was properly sensed as MTORC1 suppression in ULK1/2 DKO MEF, although LC3 conversion was not activated. In contrast, 2 hours of glucose starvation promoted AMPK activation (acetyl CoA carboxylase (ACC) phosphorylation) in wildtype (WT) MEF, but little change in MTORC1 activation. LC3-II was indeed formed following glucose starvation but independently of ULK1/2 function. We interpret this change to represent a block in lysosomal flux, as discussed later in this report (Fig 10).

To further clarify, we studied longer-term effects. MTORC1 activity recovered after overnight amino acid starvation and cells showed dramatically low total LC3 protein levels, both in WT and ULK1/2 DKO MEF (Fig 1B). In contrast, overnight glucose starvation led to mild AMPK activation and MTORC1 suppression, in both WT and ULK1/2 DKO cells. As such, cells appear to shut down MTORC1, albeit slowly, following glucose starvation, which may reflect the AMPK- or RagA-dependent glucose sensing mechanisms previously reported (25, 26). LC3-II accumulated similarly in both cell types following prolonged glucose starvation. Together, these data suggest that only amino acid starvation activates a ULK1/2-dependent immediate autophagy response. Prolonged amino acid starvation activates a further ULK1/2-independent degradative pathway that leads to LC3 clearance, ultimately leading to MTORC1 reactivation (27). As we show later in this study (Fig 10), this likely represents amino acid-starvation-based activation of the lysosome. Glucose starvation failed to robustly activate immediate or long-term autophagy degradative flux. Since MEF generally showed a

strong requirement for survival growth factors, particularly during prolonged starvation, these incubations all contained dialysed serum and only studied effects from glucose or amino acid starvation.

The complex regulatory effects of amino acid vs glucose starvation required further clarification so we tested autophagy membrane flux in MEF expressing tandem mRFP-GFP tagged LC3 (28) (Fig 2A). We confirmed that 2 hour addition of Baf A1 alone in full-nutrient conditions de-acidified and revealed all the basal autophagosomes in resting cells. Amino acid starvation of MEF for 2 hours produced mild increases in GFP-detectable (i.e. early) and RFP-detectable (i.e. total) autophagosomes. Notably, amino acid starvation produced RFP(+) only membranes, which represent autophagosomes that acidify and mature into late degradative compartments. Glucose starvation also led to mild changes in GFP- and RFP-visible membranes but the level of response was significantly less than amino acid starvation upon quantification of cell populations (Fig 2B) and did not produce RFP(+) only autophagosomes arising from flux.

In the presence of Baf A1, amino acid starvation for 2 hours led to strong accumulation of autophagosomes (visible in GFP and RFP due to global deacidification). In contrast, glucose starvation + Baf A1 produced a markedly lower level of autophagosome formation. Moreover, the amino acid starvation and Baf A1 responses at 2 hours were clearly blocked upon ULK1/2 DKO. When the experiment was performed following 18 hour starvations, we detected a distinct pattern (Fig 2B). Baf A1 alone, or both starvation conditions (+Baf A1) all led to similar accumulation of GFP(+) and RFP(+) membranes. Furthermore, this accumulation took place similarly even with ULK1/2 DKO. These results suggested that only amino-acid starvation (in the short-term) stimulated canonical autophagy flux and that this response was strictly dependent on the ULK1/2 complex. Upon prolonged (e.g. overnight) starvation, other slower-rate autophagy-related processes become more apparent but these do not display differential sensitivity to amino acid vs. glucose starvation and are ULK1/2-independent.

We further validated our findings using another imaging approach, detecting endogenous LC3-positive autophagosomes in starved WT MEF (Fig 2C). Baf A1 alone (in control conditions) only led to small accumulation of basally forming autophagosomes. LC3-positive autophagosome formation was strongly promoted by amino acid-, but not glucose-, starvation. Since, activated ULK1/2 promotes autophagy by phosphorylating downstream signalling partners such as Beclin1 (6), we further confirmed that the short-term amino-acid dependent autophagy response was blocked upon Beclin1 silencing.

Differential nutrient responses in cancer cells

The failure of glucose starvation to activate autophagy was puzzling so we investigated if this trend was conserved, particularly in cancer cells that exhibit high glucose catabolism. We found in a range of breast, ovarian and melanoma cancer cell lines that glucose starvation generally led to LC3-II accumulation, similar to cells with lysosomal inhibition via chloroquine (CQ) (Fig 3A). This similarity was most obvious in 4T1, SKOV3 and OVCAR3, but was generally displayed in the other cell types. By contrast, amino acid starvation under the same time-frame led to patterns of LC3 conversion and clearance. MCF7 and A431 were further studied as representative cell models showing clear nutrient-dependent differences. In both these cell types, overnight amino acid starvation led to strong flux and clearance of total LC3 and the sequestosome 1 /p62 autophagy adaptor protein (Fig 3B). By contrast, overnight glucose starvation did not produce strong LC3 and p62 degradation.

These results in cancer cells support our model for differential responses to amino acid vs. glucose starvation. Since changes in levels of LC3 or p62 protein can arise from both autophagy and gene expression mechanisms, particularly in prolonged starvation (29), we further tested *LC3B* and *p62/SQSTM1* transcript levels (Fig 3C). Under short-term starvation, only glucose- (but not amino acid-) starvation led to mild *LC3B* and *p62* up-regulation in MCF7 cells. A431 displayed a mild but distinct nutrient-dependent response. Under prolonged starvation, there was clearer up-regulation of LC3B and p62, particularly upon glucose starvation. The nutrient-dependent difference was especially apparent in MCF7. These data suggest that in the short term, amino acid starvation activates autophagy flux leading to loss of LC3 and p62 protein (but there is no gene down-regulation). Upon prolonged timeframes, amino acid starvation produces some up-regulation but LC3 and p62 degradation rates overwhelm. In contrast, prolonged glucose starvation does not produce degradative flux and further stimulates a *LC3* and *p62* up-regulation response. Lastly, we confirmed the differential autophagy flux by imaging A431 cells expressing mRFP-GFP-LC3 (Fig 3D,E). Similar profiles were observed, with Baf A1 (alone in control conditions) revealing basal autophagosome levels. In short-term starvation, only amino acid-, but not glucose-, starvation promoted strong autophagosome formation.

Amino acid starvation activates autophagy flux

We further investigated the nutrient-dependent regulation of autophagy using HEK293 cells, which we previously used extensively to study ULK1 signalling (30, 31). HEK293 cells

possess a high rate of basal autophagy, even under full nutrient conditions, as shown via clear LC3-II accumulation following lysosomal block with Baf A1 (Fig 4A, lane 2). Starvation of amino acid (and serum) leads to increased LC3-II (lanes 1 vs. 3) and this effect is further apparent when Baf A1 is used to block autophagic flux (lane 4). Addition of dialysed serum did not alter LC3-II accumulation (lanes 3 vs. 5) suggesting that cells were primarily sensing amino acid withdrawal. Amino acid starvation (with or without serum) strongly inhibited MTORC1. As observed above in multiple cell types, glucose (and serum) starvation led to some LC3-II formation but the extent was not as robust compared to amino acid starvation (lanes 3 vs. 6). Furthermore, glucose starvation (+Baf A1) did not produce more LC3-II as compared to Baf A1 treatment alone (also shown in quantitation (Fig 4B)). Glucose (and serum) starvation led to AMPK activation and also MTORC1 suppression. However, supplementation of dialysed serum to glucose starvation restored MTORC1 activity and prevented LC3-II generation (lanes 6 vs. 8). Therefore, starvation of just glucose alone produces minimal autophagy responses, consistent with our other data. Serum starvation can activate autophagy to a certain extent, but this contribution is weak when directly compared with amino acid starvation.

We and others have noted glucose-dependent autophagy effects, particularly following prolonged starvation (5, 11, 14, 19), so here, we investigated details in the time course of nutrient sensing. In HEK293 cells, inhibition of the lysosome led to a gradual accumulation of LC3-II over 1-4 hours (Fig 4C). Further starvation of amino acids led to significantly higher levels of rapid LC3-II formation. Glucose starvation failed to activate LC3-II formation above the low level caused by lysosomal block alone.

In these prolonged experiments, we noted mild LC3 and ACC accumulation upon overnight incubation of control cells maintained with full nutrients (Fig 4D). In contrast, amino acid starvation triggered LC3 conversion within 2 hours, becoming more clear by 4 hours, which is consistent with other data. By 18 hours of amino acid starvation, total LC3 levels markedly decreased due to continued degradation (also reflected by p62 reduction). AMPK activity remained low during amino acid starvation. The parallel time course from glucose starvation was distinct, with less LC3 conversion and clearance, no p62 loss and rapid AMPK activation.

Although different cell types display slightly varying responses, nutrient-dependent autophagy flux, as detected by RFP-GFP-LC3, has been consistent. In HEK293 cells (Fig 4E), 2 hours of Baf A1 treatment alone showed the basal autophagosome levels. Amino acid starvation produced significantly more GFP(+) and RFP(+) autophagosomes, under both +/- Baf A1 conditions.

Amino acid starvation stimulates autophagosome formation in a glucose-dependent manner

As we established the nutrient-specific effects on autophagy flux, we further studied regulation of autophagosome formation. We first investigated early autophagy factor recruitment by detecting the ULK1 complex, which translocates to initial ER-associated assembly sites. We and others have previously reported clear formation of membranes using exogenous tagged ULK1 complex members (30, 32). Here, we observed that cells maintained under full nutrients contained virtually no membranes staining for endogenous ULK1 (Fig 5A). Amino acid starvation stimulated assembly of ULK1-positive membranes within 15 minutes and further increased over time (Fig 5B). By contrast, glucose starvation did not stimulate ULK1-positive puncta.

To study a later stage of autophagosome assembly, we detected endogenous patterns of p62/Sequestosome1, which is recruited to forming autophagy membranes via both LC3-dependent and –independent mechanisms (33, 34). Amino acid starvation induced p62-positive membranes in a robust, rapid and time-dependent manner (Fig 5A,B). In contrast, glucose starvation did not induce p62 membranes. To confirm the p62 staining, we detected co-localisation with GFP-DFCP1. In WT MEF, amino acid starvation stimulated the formation of DFCP1-positive autophagosomes with concentrated patches of PtdIns3P (Fig 5C). p62 puncta co-localised with GFP-DFCP1, intermingling with the patches of PtdIns3P on autophagosomes, suggestive of cargo recruitment. The amino-acid dependent induction of p62 puncta could be blocked with the ULK1 inhibitor MRT68921 (35) (Fig 5D). Therefore, the data suggest that amino acid starvation rapidly promotes ULK1 activation and translocation, thereby promoting downstream p62 recruitment and autophagosome formation.

We further explored nutrient-dependency during autophagosome formation using p62 puncta as readout. We and others have long used Earle's balanced salt solution (EBSS) as a standard autophagy starvation medium (11, 30, 31). Notably, EBSS lacks both amino acids and serum. During the course of this study, we further clarified that serum starvation itself can mildly stimulate autophagy by suppressing MTORC1 activity (eg Fig 5A). In HEK293, we also observed that serum deprivation leads to cytoskeletal changes but determined that trace amounts of supplemented serum (0.1%) maintained cell morphology and prevented cell detachment. We confirmed that serum deprivation alone (from 10% to 0.1%) only mildly induces p62 puncta formation (Fig 5E). By comparison, further starvation of amino acid (but

not of glucose) strongly induced p62 puncta. This difference between amino acid vs. glucose starvation was observed even when starvation was performed in the context of 10% dialysed serum. Importantly, while amino acid starvation promoted p62 membranes, further removal of glucose (double-starvation) significantly blocked p62 puncta formation. We further confirmed biochemically that glucose starvation inhibited the amino acid starvation signal from promoting LC3 lipidation (Fig 6A). Therefore, glucose starvation blocked the otherwise strong induction from amino acid starvation for autophagosome formation.

Since amino acid and glucose starvation were having opposite effects on autophagy, we asked how these nutrients were being sensed. As expected, glucose starvation led to AMPK activation and strong phosphorylation of ACC (Fig 6B). This condition also increased phosphorylation of ULK1-Ser555. By contrast, amino acid starvation led to suppression of MTORC1 signalling without strong AMPK activation (P-ACC). Under amino acid starvation, we observed, as expected, decreased phosphorylation on ULK1-Ser757, but also decreased phospho-ULK1-Ser555. Interestingly, double starvation of both amino acid and glucose led to MTORC1 inhibition together with AMPK activation, restoring ULK1-Ser555 phosphorylation. The other AMPK-regulated site, ULK1-Ser317 (5), showed generally steady levels throughout these starvation conditions. Altogether, these data show that maximal autophagy activation is associated with dephosphorylation on both the ULK1-Ser555 and Ser757 sites.

Glutamine, leucine and arginine activate MTORC1 to inhibit autophagosome formation

All data above highlighted the primacy of amino acids for autophagy regulation. Certain amino acids, such as glutamine, leucine and arginine play key regulatory roles by interacting with specific cellular nutrient sensors to activate MTORC1 (36-39). Here, we further tested roles of each of these key regulatory amino acids. In control samples, HEK293 cells starved of all 20 amino acids showed MTORC1 suppression and LC3 lipidation (Fig 6C). However, addback of glutamine + leucine + arginine to the starvation mixture prevented both MTORC1 inactivation and LC3 lipidation. Interestingly, addback of glutamine, leucine or arginine each singly did not have strong reversal effect as compared to all three regulatory amino acids added together. Combination of leucine and arginine addback did reduce autophagy, but not as clearly as the three combined regulatory amino acids. Addback of these regulatory amino acids required the presence of serum to activate MTORC1 and suppress autophagy (data not shown), revealing involvement of the growth factor-TSC1/2-Rheb pathway in combination with amino acid for MTORC1 activation.

We confirmed that addback of glutamine + leucine + arginine to the amino acid deprivation media also suppressed formation of p62-positive autophagosomes (Fig 6D,E). To further test the ability of these 3 regulatory amino acids to control autophagy, we studied membrane translocation. We confirmed that addback of glutamine + leucine + arginine (in the presence of serum) stimulated within 10 min the translocation of MTORC1 onto lysosomal compartments (Fig 7A). To study the regulation of initiation, we monitored ULK1/2 complex localisation. We confirmed translocation of endogenous ULK1 onto membrane puncta within ~2 hours (Fig 7B). Sites of initiation, likely connected to the ER, were generally juxtaposed but not co-localised to the lysosomal compartments. Addback of glutamine + leucine + arginine caused ULK1 translocation off membrane puncta within 10 min, suggestive of rapid inactivation by the addition of regulatory amino acids. Staining for endogenous ATG13 showed identical results (Fig 7C).

AMPK phosphorylates and inhibits ULK1

We determined above that glucose starvation has the ability to suppress autophagy, even in the context of amino acid starvation cues, which promotes the process. To investigate this mechanism further, we focussed on AMPK which is activated by glucose starvation. To use a different approach, we used the compound A769662 activate AMPK (40). A769662 clearly activated AMPK under both full-nutrient and amino-acid starvation conditions (Fig 8A). There was no adverse effects of A769662 on the MTORC1 pathway. We next tested the effect of AMPK activation on amino acid starvation-driven autophagy flux using the RFP-GFP-LC3 assay in HEK293 cells. The addition of A769662 significantly inhibited both basal autophagosome formation under full-nutrients and autophagy stimulate by amino acid starvation (Fig 8B,C). The effect of the AMPK activator was nearly identical to the effect of glucose withdraw on amino acid starvation (i.e. double starvation) (Fig 8D). The addition of A769662 similarly inhibited the ability of amino acid starvation to promote ULK1 and p62 puncta formation (Fig 9A). These results support the notion that AMPK inhibits autophagy.

AMPK regulates autophagy by directly phosphorylating ULK1 on multiple sites. One set of highly conserved sites (mouse ULK1 S467, S555, T574, S637) has been implicated in autophagy-related mitochondrial homeostasis and cell survival (9). To test the roles of these AMPK-dependent sites, we reconstituted ULK1/2 DKO MEF with either ULK1 WT or the 4SA (S467A, S555A, T574A, S637A) mutant (Fig 9B). We next treated the reconstituted MEF to amino acid starvation +/- AMPK activation via A769662 and monitored p62-labeled autophagosome formation (Fig 9C,D). Reconstitution with WT-ULK1 rescued the formation of starvation-induced p62 puncta. This autophagy response in WT-ULK1 reconstituted MEF was significantly inhibited by A769662. Interestingly, MEF reconstituted with 4SA-ULK1

showed a significantly inhibited response to amino acid starvation. A pattern consistent with this was also observed when studying WT vs. 4SA reconstituted MEF in the context of single (-AA) vs. double (-AA-Glc) starvation (Fig 9E). Therefore, phosphorylation of these 4 sites on ULK1 was required for AMPK to inhibit the autophagy response. However, loss of these sites also impaired the normal function of ULK1 during amino acid starvation-induced autophagy.

AMPK and glucose starvation inhibit lysosome activity

Our data above highlighted how amino acid starvation was best at activating autophagy-lysosomal flux as seen through eventual clearance of LC3 and p62 proteins. Since MTORC1-dependent activation of lysosomal activity has been reported (41), we investigated the differential nutrient dependency on this late stage of autophagy. We confirmed that amino acid starvation led to robust lysosomal activation in HEK293 and HeLa cells as detected by lysotracker red staining for acidified vesicles (Fig 10A). Quantification of staining indicated starvation-induced lysosomal acidification, which could be effectively quenched by treatment with weak base CQ or more strongly, with vaculolar ATPase (vATPase) inhibitor Baf A1 (Fig 10B), as seen elsewhere (29).

In testing the different nutrients, we found that serum starvation alone led to mild acidification of the lysosome, for example in both HeLa (Fig 10C,D) and HEK293 cells (Fig 10E). However, further withdrawal of amino acids markedly led to strong lysosomal acidification. In contrast, glucose starvation did not promote acidification. We found that the preferential lysosomal activation from amino acid starvation was independent of autophagy, showing similar robust effects in WT and ATG5 KO MEF (Fig 10F,G). Lysosomes in ATG5KO MEF appeared swollen compared to those in WT. However, even these swollen vesicles markedly increased lysotracker staining following amino acid starvation. The ability of amino acid starvation to activate lysosomal acidification was also independent of the ULK1 signalling, as seen in ULK1/2DKO and FIP200 KO MEF (Fig 10H).

Our data above also highlighted how glucose starvation inhibited amino acid-dependent cues that drive autophagosome formation. We tested this relationship for lysosomal acidification. Indeed, we found that while amino acid starvation stimulated lysosomes, acidification was blocked when glucose was further removed using double starvation medium (Fig 10I). Addback of glucose to the double starvation medium (to typical levels: 1 g/L) restored acidification, indicating that cellular glucose levels promote lysosomal function. As one main effect, glucose starvation activates AMPK. To test if this pathway regulates the lysosome, we used the AMPK activator drug. Addition of A769662 had little effect on basal

365 signals, but significantly inhibited the ability of amino acid starvation to promote lysosome
366 acidification (Fig 10J-L). These results suggest that glucose starvation also inhibits
367 lysosomal / late-stage autophagy via AMPK.

368

Discussion

Mammalian cells need to rapidly adapt when extracellular nutrients change and a part of this metabolic homeostasis is autophagy (1, 42). Cancer cells are particularly distinct for their re-configured metabolic profile that features high consumption of glucose and amino acids such as glutamine (43, 44). In this regard, we have long been intrigued by the mechanisms linking amino acid and glucose sensing to autophagy, particularly in cancer contexts. ULK1 appears to be a key hub receiving phosphorylation signals from MTORC1 and AMPK (5, 10). We previously investigated the different features of non-canonical ULK1/2-independent autophagy in the context of prolonged glucose starvation (11, 14). Here, upon further exploration, we find surprisingly that only amino acid starvation activates rapid and robust autophagy flux. In contrast, glucose starvation produced autophagy readouts more resembling a lysosomal block, which was prevalent in a wide range of normal and cancer cell types.

Amino acid and glucose differentially control autophagosome formation

Differences in nutrient sensing could be traced to the level of autophagy initiation. Only amino acid starvation promptly promoted and translocation of ULK1 to membrane assembly sites. This is likely the key early regulatory event that allows phosphorylation downstream substrates such as ATG4B, ATG9 and ATG13 (35, 45-48). This is clearly a partial list of all the ULK1 substrates so far identified (as previously highlighted (7, 49)). However, this translocation critically allows the ULK1/2 complex to phosphorylate Beclin1 thereby directing VPS34 activity and localised PtdIns3P generation at autophagosome assembly sites (6). Previously, we found only amino acid starvation stimulated translocation of PtdIns3P-binding WIPI-2 to autophagy membranes (11). In further agreement, we here found that amino acid (but not glucose) starvation rapidly promoted high numbers of autophagosomes containing LC3 and p62. Consistent with established thinking, MTORC1 played the predominant role for autophagosome regulation. Re-addition of key regulatory amino acids glutamine, leucine and arginine to starved cells re-activated MTORC1 and blocked the autophagy. Thus, the main 3 regulatory amino acids are sufficient to control autophagosome assembly.

When considering autophagy and the different nutrients, our data highlighted how time was a key variable. The clearest differences between amino acid vs. glucose starvation were observed during the immediate rapid autophagy response (e.g. up to 2 hours). Therefore, amino acid-dependent MTORC1-ULK1 signalling thus serves to primarily promote rapid high rates of LC3 conversion and autophagosome assembly. During prolonged starvation experiments, we observed other ULK1/2-independent pathways, which we interpret to

function at lower rates, becoming apparent in longer timeframes. Cellular LC3 levels are effectively cleared upon prolonged amino acid starvation, likely reflecting sustained activation of lysosomal function. Basal autophagosome formation was seen to be ULK1/2-independent after prolonged block of flux (i.e. Baf A1). Serum starvation also produced mild effects on autophagosome formation, MTORC1 activity and lysosomal acidification. We suggest that considerations of timeframe and serum levels may explain some of the observations on glucose starvation-induced, non-canonical, ULK1/2-independent autophagy (5, 14, 17, 19). Overall, amino acid and glucose starvation produced clearly different effects across many cell types.

AMPK and glucose starvation signals can dominate and block autophagy

Interestingly, while amino acid starvation stimulated autophagy, further removal of glucose in the amino acid-free condition blocked autophagosome formation. Previously, it had been proposed that autophagy initiation in both mammalian and yeast cells require threshold levels of cellular energy (20, 23, 50). Glucose starvation in our experiments clearly reduced the energy charge in cells as reflected by AMPK activation and phosphorylation of the ULK1-Ser555 site. Altogether, highest levels of autophagy were associated with amino acid deprivation and hypo-phosphorylation of ULK1 at Ser555 and Ser757. As such, canonical rapid autophagy seems to be driven by suppression of MTORC1 in association with low AMPK activity.

We were next able to show that activation of AMPK using a drug was able to suppress the otherwise positive signal of amino acid starvation for autophagosome formation. This brake mechanism on autophagy appears to require the set of 4 conserved AMPK phosphorylation sites on ULK1 (including Ser555), which had been previously validated functionally (9). Therefore, high levels of AMPK-mediated phosphorylation on these sites may serve to inhibit ULK1. However, the relationship is not binary since 4SA mutation of these sites also prevented ULK1 from promoting normal autophagy. One possibility is that transient or sub-threshold levels of AMPK phosphorylation on these sites is needed for proper dynamic regulation of ULK1. Sustained high levels of modification may serve as a signal to block ULK1. Alternatively, one of the sites in this set may function as the brake but the 4SA substitutions together may inhibit other positive roles although this will require more mapping. Indeed, one of the sites in 4SA is Ser637 (638 in human), which is also coordinately regulated by MTORC1 and PP2A in response to nutrients (10, 51). ULK1-Ser555 phosphorylation may provide a switch from canonical autophagy to mitophagy-specific pathways following AMPK activation (8, 9).

Amino acid and glucose differentially control the lysosome

We consistently saw that amino acid starvation, especially when prolonged, generated LC3 conversion, LC3 breakdown and MTORC1 reactivation. By contrast, glucose starvation led to only slow accumulation of lipidated LC3-II and never re-stimulated MTORC1, which we interpreted to reflect overall lysosomal suppression. This model suggests further considerations that may explain the LC3 accumulation observed in other examples of glucose starvation (5, 14, 17, 19).

Autophagy flux depends on fusion with the lysosome to enable content degradation. Lysosomal function can be up-regulated following gene expression re-programming and organelle biogenesis driven by TFEB family transcription factors (52). Alternatively, existing lysosomes can be activated by promoting lumenal acidification, which has been reported via both MTORC1-dependent and -independent mechanisms (41, 53). Here, we found that serum starvation promoted some acidification but strongest lysosomal activation occurred when both serum and amino acids were withdrawn. This lysosomal response occurred rapid and independently of the ATG5 and ULK1/2 autophagy pathways. Glucose starvation did not stimulate lysosomal acidification, consistent with the other data suggesting low autophagic flux. Looking at nutrient combinations, removal of glucose prevented amino acid and serum starvation from promoting lysosome acidification. Furthermore, activation of AMPK was sufficient to suppress lysosomal activation. Therefore, AMPK has ULK1-dependent pathways to control early autophagy steps and distinct pathways to control the lysosome.

Lysosomal acidification is driven by vATPase, which interestingly displays nutrient-dependent assembly of its V0 and V1 domains (54). Starvation of amino acids has been shown to promote vATPase assembly, although roles of MTORC1 in this mechanism remain controversial (41, 53, 55). Conversely, vATPase assembly has been shown in yeast and mammals to require glucose (56, 57). Here, we identify an additional pathway involving AMPK activity to suppress lysosomal function. Therefore, vATPase may be blocked via multiple mechanisms to produce a reduction in autophagy-lysosomal flux upon glucose starvation.

In conclusion, our studies provide an integrated view on how serum, amino acid and glucose independently control early and late stages of autophagy. For both autophagosome formation and lysosomal acidification, amino acid starvation provided the strongest activating signal. Surprisingly, both early and late stages of autophagy were not activated by glucose starvation and moreover, glucose starvation had overall inhibitory effects on both pathways.

The inhibitory effects of glucose starvation were determined to take place via distinct AMPK-dependent mechanisms on autophagy initiation and lysosomal activity. The mechanisms characterised here may help coordinate the physiological homeostasis of amino acids, glucose and autophagy, as seen in neonatal mice (26). Our findings here also illustrate that different nutrient starvations cannot all be generalised to activate autophagy.

Materials and Methods

Cell culture and treatments

ULK1/2 DKO MEF (11); WT MEF expressing GFP-DFCP1 (ZFYVE1) (11); FIP200 KO (58) and ATG5 KO MEF (and matched WT) (59) have been described. HEK293A cells were maintained as previously described (31). MEF, HEK293A, HeLa, 4T1, SKOV3, OVCAR, B16-F0 and A431 were all maintained in DMEM with 4.5g/L glucose (Lonza #BE12-614F) supplemented with 10% fetal bovine serum (FBS) (Labtech #FCS-SA), 4mM L-Glutamine (Lonza #BE17-605E), and 100U/mL Penicillin/Streptomycin (Lonza #DE17-602E) (full-nutrient media). MCF7 were cultured in full-nutrient media supplemented with 0.015 mg/ml insulin.

Where indicated, WT and ULK1/2 DKO MEF were transiently transfected with tandem tagged mRFP-EGFP-LC3 reporter (28). Alternatively, HEK293A and A431 cell lines were generated stably expressing pBABE-puro mCherry-EGFP-LC3B (Addgene plasmid # 22418)(60). A HEK293A stable cell line was generated expressing LAMP1-mRFP-FLAG (Addgene plasmid # 34611) (61). MEF with stable knockdown of Beclin1 were generated using the pLKO.1 construct for mouse BECN1 clone id: TRCN0000087290. In reconstitution experiments, ULK1/2 DKO MEF were stably transduced using pLPC puro-Myc-ULK1 WT or 4SA (S467A, S555A, T574A, S637A) (subcloned from Addgene plasmids # 27626 and 27628) (9).

Cells were washed 1x with PBS and exchanged into starvation media. For amino (and serum) starvation, we used Earle's balanced salt solution (EBSS) (Sigma E2888). For glucose (and serum) starvation, we used glucose-free DMEM media containing 4mM L-Glutamine (Thermo Fisher 11966-025). For serum starvation, used full-nutrient DMEM described above but lacking FBS. For amino acid and glucose (double) starvation, we used PBS (Lonza #BE17-513F) supplemented with 0.22% sodium bicarbonate (Sigma S8761) and phenol red. To study glucose addback, we used PBS containing 1 g/L glucose (Lonza #04-479Q) supplemented with 0.22% sodium bicarbonate and phenol red. Where indicated,

dialysed FBS (Sigma F0392) was supplemented. Where indicated 4 mM glutamine (Lonza #BE17-605E), 0.8 mM leucine (Sigma L8912) and 0.4 mM arginine (Sigma A8094) were supplemented. Some conditions used 10nM Bafilomycin A1 (Tocris Bioscience) or 25μM chloroquine (Sigma) to inhibit the lysosome. AMPK was activated using 50 μM A769662 (Tocris Bioscience). MRT68921 (35) was a kind gift from B. Saxty (LifeArc, formerly MRC Technology).

Immunoblot analysis

Cell lysates were prepared as described previously (11) and analysed using on 4-12% or 10% NuPAGE gels resolved in MES running buffer (Thermo Fisher scientific). Membranes were stained using the following antibodies. LC3B: clone 5F10 (Nanotools #0231-100); p62/SQSTM1 (BD Bioscience 610832); phospho-S6 ser240/244 (Cell signalling 2215); total S6 (54D2) Mouse mAb (Cell signalling 2317); phospho-acetyl CoA carboxylase (ACC) ser79 (Cell signalling 3661); total ACC (Cell signalling 3662); phospho-ULK1 ser757 (Cell signalling 6888); phospho-ULK1 ser555-D1H4 (Cell signalling 5869); phospho-ULK1 ser317-D2B6Y (Cell signalling 12753); total ULK1-D8H5 (Cell signalling 8054); Actin: Ab-5 (BD Bioscience # 612656). Detection was via anti-mouse or anti-rabbit Dylight-coupled secondary antibodies and Licor Odyssey infrared scanning.

Microscopy

After treatments, cells were fixed and stained using the following antibodies: anti-human p62/SQSTM1 (BD Bioscience 610832); anti-mouse p62/SQSTM1 Guinea pig polyclonal (Progen #GP62-C); LC3B (Cell signalling 2775); MTOR-7C10 (Cell signalling 2983); ATG13- E1Y9V (Cell signalling 13468); ULK1-D8H5. Cell images were captured by confocal microscopy (Leica, TCS SP5, HCX PL APO CS-63x-1.4NA objective and HyD GaAsP detection). Puncta/cell were quantified from confocal scans or directly by epifluorescent imaging, depending on stain. To detect lysosomal acidification, cells were treated as indicated with 50nM Lysotracker Red DND-99 (Thermo Fisher L7528) added during the final 30mins of incubation. Cells were fixed with paraformaldehyde, stored overnight, and imaged by confocal microscopy. Staining intensity was quantified from cytoplasmic regions of interest from multiple cells per field from multiple fields per sample. Quantification of autophagosome puncta and lysotracker staining representative of multiple experiments as detailed in legends.

Transcript analysis

RNA was extracted from cells using ISOLATE II RNA Mini columns (Bioline). Expression analysis was carried out using the Luna One-Step RT-qPCR kit and the following primers: Hs *LC3B*: forward ACG CAT TTG CCA TCA CAG TTG; reverse TCT CTT AGG AGT CAG GGA CCT TCA G; Hs *p62/SQSTM1*: forward CCG TGA AGG CCT ACC TTC TG; reverse TCC TCG TCA CTG GAA AAG GC; Hs *GAPDH*: forward CTA TAA ATT GAG CCC GCA GCC; reverse ACC AAA TCC GTT GAC TCC GA. Gene fold-change normalised to *GAPDH* was calculated using double-delta Ct analysis.

Statistics

Quantitative data were managed using GraphPad Prism and Origin Pro; and analysed using unpaired T-test (for 2-way comparisons) or one-way ANOVA with Tukey post-test (multiple comparisons) as appropriate. In box whisker plots, boxes show 25th, 75th percentiles and mean. Whiskers show standard deviation. (X) indicate 1st and 99th percentiles.

Acknowledgements

CN was supported by a National Open University of Nigeria, Tertiary Education Trust Fund (TETFund). LW was supported by a doctoral centre studentship from the Biotechnology and Biological Sciences Research Council (BBSRC) UK. LG was supported by a studentship from Cancer Research UK Glasgow Centre. JG was supported by NIH grant NS094144. The funders had no role in study design, data collection and interpretation, or the decision to submit the work for publication. We thank N. Mizushima (University of Tokyo) for ATG5KO MEF. We thank the following for sharing constructs: T. Yoshimori (Osaka University) mRFP-EGFP-LC3; J. Debnath (University of California San Francisco) pBABE-puro mCherry-EGFP-LC3B; D. Sabatini (MIT Whitehead Institute) LAMP1-mRFP-FLAG; R. Shaw (Salk Institute for Biological Studies) Myc-ULK1 WT and 4SA.

Conflicts of interest

The authors have no competing financial interests.

References

1. **Galluzzi L, Pietrocola F, Levine B, Kroemer G.** 2014. Metabolic control of autophagy. Cell **159:**1263-1276.
2. **Guo JY, Teng X, Laddha SV, Ma S, Van Nostrand SC, Yang Y, Khor S, Chan CS, Rabinowitz JD, White E.** 2016. Autophagy provides metabolic substrates to maintain energy charge and nucleotide pools in Ras-driven lung cancer cells. Genes Dev **30:**1704-1717.
3. **Kamada Y, Funakoshi T, Shintani T, Nagano K, Ohsumi M, Ohsumi Y.** 2000. Tor-mediated induction of autophagy via an Apg1 protein kinase complex. J Cell Biol **150:**1507-1513.
4. **White E.** 2015. The role for autophagy in cancer. J Clin Invest **125:**42-46.
5. **Kim J, Kundu M, Viollet B, Guan KL.** 2011. AMPK and mTOR regulate autophagy through direct phosphorylation of Ulk1. Nat Cell Biol **13:**132-141.
6. **Russell RC, Tian Y, Yuan H, Park HW, Chang YY, Kim J, Kim H, Neufeld TP, Dillin A, Guan KL.** 2013. ULK1 induces autophagy by phosphorylating Beclin-1 and activating VPS34 lipid kinase. Nat Cell Biol **15:**741-750.
7. **Egan DF, Chun MG, Vamos M, Zou H, Rong J, Miller CJ, Lou HJ, Raveendra-Panickar D, Yang CC, Sheffler DJ, Teriete P, Asara JM, Turk BE, Cosford ND, Shaw RJ.** 2015. Small Molecule Inhibition of the Autophagy Kinase ULK1 and Identification of ULK1 Substrates. Mol Cell **59:**285-297.
8. **Tian W, Li W, Chen Y, Yan Z, Huang X, Zhuang H, Zhong W, Chen Y, Wu W, Lin C, Chen H, Hou X, Zhang L, Sui S, Zhao B, Hu Z, Li L, Feng D.** 2015. Phosphorylation of ULK1 by AMPK regulates translocation of ULK1 to mitochondria and mitophagy. FEBS Lett **589:**1847-1854.
9. **Egan DF, Shackelford DB, Mihaylova MM, Gelino S, Kohnz RA, Mair W, Vasquez DS, Joshi A, Gwinn DM, Taylor R, Asara JM, Fitzpatrick J, Dillin A, Viollet B, Kundu M, Hansen M, Shaw RJ.** 2011. Phosphorylation of ULK1 (hATG1) by AMP-activated protein kinase connects energy sensing to mitophagy. Science **331:**456-461.
10. **Shang L, Chen S, Du F, Li S, Zhao L, Wang X.** 2011. Nutrient starvation elicits an acute autophagic response mediated by Ulk1 dephosphorylation and its subsequent dissociation from AMPK. Proc Natl Acad Sci U S A **108:**4788-4793.
11. **McAlpine F, Williamson LE, Tooze SA, Chan EY.** 2013. Regulation of nutrient-sensitive autophagy by uncoordinated 51-like kinases 1 and 2. Autophagy **9:**361-373.
12. **Tsuboyama K, Koyama-Honda I, Sakamaki Y, Koike M, Morishita H, Mizushima N.** 2016. The ATG conjugation systems are important for degradation of the inner autophagosomal membrane. Science **354:**1036-1041.
13. **Karanasios E, Walker SA, Okkenhaug H, Manifava M, Hummel E, Zimmermann H, Ahmed Q, Domart M-C, Collinson L, Ktistakis NT.** 2016. Autophagy initiation by ULK complex assembly on ER tubulovesicular regions marked by ATG9 vesicles. Nat Commun **7**.
14. **Cheong H, Lindsten T, Wu J, Lu C, Thompson CB.** 2011. Ammonia-induced autophagy is independent of ULK1/ULK2 kinases. Proc Natl Acad Sci U S A **108:**11121-11126.
15. **Mrschtik M, O'Prey J, Lao LY, Long JS, Beaumatin F, Strachan D, O'Prey M, Skommer J, Ryan KM.** 2015. DRAM-3 modulates autophagy and promotes cell survival in the absence of glucose. Cell Death Differ **22:**1714-1726.
16. **Vicinanza M, Korolchuk VI, Ashkenazi A, Puri C, Menzies FM, Clarke JH, Rubinsztein DC.** 2015. PI(5)P regulates autophagosome biogenesis. Mol Cell **57:**219-234.
17. **Gammoh N, Florey O, Overholtzer M, Jiang X.** 2013. Interaction between FIP200 and ATG16L1 distinguishes ULK1 complex-dependent and -independent autophagy. Nat Struct Mol Biol **20:**144-149.
18. **Chang C, Su H, Zhang D, Wang Y, Shen Q, Liu B, Huang R, Zhou T, Peng C, Wong CC, Shen HM, Lippincott-Schwartz J, Liu W.** 2015. AMPK-Dependent Phosphorylation of GAPDH Triggers Sirt1 Activation and Is Necessary for Autophagy upon Glucose Starvation. Mol Cell **60:**930-940.

19. **Roberts DJ, Tan-Sah VP, Ding EY, Smith JM, Miyamoto S.** 2014. Hexokinase-II positively regulates glucose starvation-induced autophagy through TORC1 inhibition. Mol Cell **53:**521-533.
20. **Plomp PJ, Wolvetang EJ, Groen AK, Meijer AJ, Gordon PB, Seglen PO.** 1987. Energy dependence of autophagic protein degradation in isolated rat hepatocytes. Eur J Biochem **164:**197-203.
21. **Samari HR, Seglen PO.** 1998. Inhibition of hepatocytic autophagy by adenosine, aminoimidazole-4-carboxamide riboside, and N6-mercaptopurine riboside. Evidence for involvement of amp-activated protein kinase. J Biol Chem **273:**23758-23763.
22. **Ravikumar B, Stewart A, Kita H, Kato K, Duden R, Rubinsztein DC.** 2003. Raised intracellular glucose concentrations reduce aggregation and cell death caused by mutant huntingtin exon 1 by decreasing mTOR phosphorylation and inducing autophagy. Hum Mol Genet **12:**985-994.
23. **Moruno-Manchon JF, Perez-Jimenez E, Knecht E.** 2013. Glucose induces autophagy under starvation conditions by a p38 MAPK-dependent pathway. Biochem J **449:**497-506.
24. **Ramirez-Peinado S, Leon-Annicchiarico CL, Galindo-Moreno J, Iurlaro R, Caro-Maldonado A, Prehn JH, Ryan KM, Munoz-Pinedo C.** 2013. Glucose-starved cells do not engage in prosurvival autophagy. J Biol Chem **288:**30387-30398.
25. **Shaw RJ, Bardeesy N, Manning BD, Lopez L, Kosmatka M, DePinho RA, Cantley LC.** 2004. The LKB1 tumor suppressor negatively regulates mTOR signaling. Cancer Cell **6:**91-99.
26. **Efeyan A, Zoncu R, Chang S, Gumper I, Snitkin H, Wolfson RL, Kirak O, Sabatini DD, Sabatini DM.** 2013. Regulation of mTORC1 by the Rag GTPases is necessary for neonatal autophagy and survival. Nature **493:**679-683.
27. **Yu L, McPhee CK, Zheng L, Mardones GA, Rong Y, Peng J, Mi N, Zhao Y, Liu Z, Wan F, Hailey DW, Oorschot V, Klumperman J, Baehrecke EH, Lenardo MJ.** 2010. Termination of autophagy and reformation of lysosomes regulated by mTOR. Nature **465:**942-946.
28. **Kimura S, Noda T, Yoshimori T.** 2007. Dissection of the autophagosome maturation process by a novel reporter protein, tandem fluorescent-tagged LC3. Autophagy **3:**452-460.
29. **Sahani MH, Itakura E, Mizushima N.** 2014. Expression of the autophagy substrate SQSTM1/p62 is restored during prolonged starvation depending on transcriptional upregulation and autophagy-derived amino acids. Autophagy **10:**431-441.
30. **Chan EY, Kir S, Tooze SA.** 2007. siRNA screening of the kinome identifies ULK1 as a multidomain modulator of autophagy. J Biol Chem **282:**25464-25474.
31. **Chan EY, Longatti A, McKnight NC, Tooze SA.** 2009. Kinase-inactivated ULK proteins inhibit autophagy via their conserved C-terminal domains using an Atg13-independent mechanism. Mol Cell Biol **29:**157-171.
32. **Itakura E, Mizushima N.** 2010. Characterization of autophagosome formation site by a hierarchical analysis of mammalian Atg proteins. Autophagy **6:**764-776.
33. **Itakura E, Mizushima N.** 2011. p62 Targeting to the autophagosome formation site requires self-oligomerization but not LC3 binding. J Cell Biol **192:**17-27.
34. **Pankiv S, Clausen TH, Lamark T, Brech A, Bruun JA, Outzen H, Overvatn A, Bjorkoy G, Johansen T.** 2007. p62/SQSTM1 binds directly to Atg8/LC3 to facilitate degradation of ubiquitinated protein aggregates by autophagy. J Biol Chem **282:**24131-24145.
35. **Petherick KJ, Conway OJ, Mpamhanga C, Osborne SA, Kamal A, Saxty B, Ganley IG.** 2015. Pharmacological inhibition of ULK1 kinase blocks mammalian target of rapamycin (mTOR)-dependent autophagy. J Biol Chem **290:**11376-11383.
36. **Lim CY, Zoncu R.** 2016. The lysosome as a command-and-control center for cellular metabolism. J Cell Biol **214:**653-664.
37. **Jewell JL, Kim YC, Russell RC, Yu FX, Park HW, Plouffe SW, Tagliabracci VS, Guan KL.** 2015. Metabolism. Differential regulation of mTORC1 by leucine and glutamine. Science **347:**194-198.

38. **Chantranupong L, Scaria SM, Saxton RA, Gygi MP, Shen K, Wyant GA, Wang T, Harper JW, Gygi SP, Sabatini DM.** 2016. The CASTOR Proteins Are Arginine Sensors for the mTORC1 Pathway. Cell **165:**153-164.
39. **Carroll B, Maetzel D, Maddocks OD, Otten G, Ratcliff M, Smith GR, Dunlop EA, Passos JF, Davies OR, Jaenisch R, Tee AR, Sarkar S, Korolchuk VI.** 2016. Control of TSC2-Rheb signaling axis by arginine regulates mTORC1 activity. Elife **5**.
40. **Göransson O, McBride A, Hawley SA, Ross FA, Shpiro N, Foretz M, Viollet B, Hardie DG, Sakamoto K.** 2007. Mechanism of Action of A-769662, a Valuable Tool for Activation of AMP-activated Protein Kinase. Journal of Biological Chemistry **282:**32549-32560.
41. **Zhou J, Tan SH, Nicolas V, Bauvy C, Yang ND, Zhang J, Xue Y, Codogno P, Shen HM.** 2013. Activation of lysosomal function in the course of autophagy via mTORC1 suppression and autophagosome-lysosome fusion. Cell Res **23:**508-523.
42. **Chantranupong L, Wolfson RL, Sabatini DM.** 2015. Nutrient-sensing mechanisms across evolution. Cell **161:**67-83.
43. **Vander Heiden MG.** 2011. Targeting cancer metabolism: a therapeutic window opens. Nat Rev Drug Discov **10:**671-684.
44. **Vazquez A, Kamphorst JJ, Markert EK, Schug ZT, Tardito S, Gottlieb E.** 2016. Cancer metabolism at a glance. J Cell Sci **129:**3367-3373.
45. **Pengo N, Agrotis A, Prak K, Jones J, Ketteler R.** 2017. A reversible phospho-switch mediated by ULK1 regulates the activity of autophagy protease ATG4B. Nat Commun **8:**294.
46. **Papinski D, Schuschnig M, Reiter W, Wilhelm L, Barnes CA, Maiolica A, Hansmann I, Pfaffenwimmer T, Kijanska M, Stoffel I, Lee SS, Brezovich A, Lou JH, Turk BE, Aebersold R, Ammerer G, Peter M, Kraft C.** 2014. Early steps in autophagy depend on direct phosphorylation of Atg9 by the Atg1 kinase. Mol Cell **53:**471-483.
47. **Mack HI, Zheng B, Asara JM, Thomas SM.** 2012. AMPK-dependent phosphorylation of ULK1 regulates ATG9 localization. Autophagy **8:**1197-1214.
48. **Joo JH, Dorsey FC, Joshi A, Hennessy-Walters KM, Rose KL, McCastlain K, Zhang J, Iyengar R, Jung CH, Suen DF, Steeves MA, Yang CY, Prater SM, Kim DH, Thompson CB, Youle RJ, Ney PA, Cleveland JL, Kundu M.** 2011. Hsp90-Cdc37 chaperone complex regulates Ulk1- and Atg13-mediated mitophagy. Mol Cell **43:**572-585.
49. **Gallagher L, Williamson L, Chan E.** 2016. Advances in Autophagy Regulatory Mechanisms. Cells **5:**24.
50. **Lang MJ, Martinez-Marquez JY, Prosser DC, Ganser LR, Buelto D, Wendland B, Duncan MC.** 2014. Glucose starvation inhibits autophagy via vacuolar hydrolysis and induces plasma membrane internalization by down-regulating recycling. J Biol Chem **289:**16736-16747.
51. **Wong PM, Feng Y, Wang J, Shi R, Jiang X.** 2015. Regulation of autophagy by coordinated action of mTORC1 and protein phosphatase 2A. Nat Commun **6:**8048.
52. **Settembre C, Fraldi A, Medina DL, Ballabio A.** 2013. Signals from the lysosome: a control centre for cellular clearance and energy metabolism. Nat Rev Mol Cell Biol **14:**283-296.
53. **Cai W, Wei Y, Jarnik M, Reich J, Lilly MA.** 2016. The GATOR2 Component Wdr24 Regulates TORC1 Activity and Lysosome Function. PLoS Genet **12:**e1006036.
54. **Cotter K, Stransky L, McGuire C, Forgac M.** 2015. Recent Insights into the Structure, Regulation, and Function of the V-ATPases. Trends Biochem Sci **40:**611-622.
55. **Stransky LA, Forgac M.** 2015. Amino Acid Availability Modulates Vacuolar H+-ATPase Assembly. J Biol Chem **290:**27360-27369.
56. **Sautin YY, Lu M, Gaugler A, Zhang L, Gluck SL.** 2005. Phosphatidylinositol 3-kinase-mediated effects of glucose on vacuolar H+-ATPase assembly, translocation, and acidification of intracellular compartments in renal epithelial cells. Mol Cell Biol **25:**575-589.
57. **Kane PM.** 2012. Targeting reversible disassembly as a mechanism of controlling V-ATPase activity. Curr Protein Pept Sci **13:**117-123.

58. **Gan B, Peng X, Nagy T, Alcaraz A, Gu H, Guan JL.** 2006. Role of FIP200 in cardiac and liver development and its regulation of TNFalpha and TSC-mTOR signaling pathways. J Cell Biol **175:**121-133.

59. **Kuma A, Hatano M, Matsui M, Yamamoto A, Nakaya H, Yoshimori T, Ohsumi Y, Tokuhisa T, Mizushima N.** 2004. The role of autophagy during the early neonatal starvation period. Nature **432:**1032-1036.

60. **N'Diaye EN, Kajihara KK, Hsieh I, Morisaki H, Debnath J, Brown EJ.** 2009. PLIC proteins or ubiquilins regulate autophagy-dependent cell survival during nutrient starvation. EMBO Rep **10:**173-179.

61. **Zoncu R, Bar-Peled L, Efeyan A, Wang S, Sancak Y, Sabatini DM.** 2011. mTORC1 senses lysosomal amino acids through an inside-out mechanism that requires the vacuolar H(+)-ATPase. Science **334:**678-683.

Figure 1. Glucose starvation does not activate autophagy flux.

(A) Wildtype or ULK1/2 double knockout (DKO) MEF were exposed to glucose starvation (-Glc), in the presence of Bafilomycin A1 (Baf A1) as indicated for 2 or 18hrs. Starvation conditions contained 10% dialysed FBS. Cell lysates were analysed for LC3B lipidation and quantified as LC3-II/LC3-I (n=3 experiments +/-SEM). Two different lines of ULK1/2 DKO MEF were analysed.

(B) Cells were exposed to amino acid (-AA) or glucose starvation for the incubated times. Starvation conditions contained 10% dialysed FBS. Cell lysates were analysed for LC3B, phospho- or total acetyl CoA carboxylase (ACC); and phospho- or total ribosomal S6 (S6). Quantification from n=3 experiments (+/-SEM). P< (*) 0.05; (**) 0.01; (***) 0.001; (****) 0.0001 by T-test.

Figure 2. Amino acid starvation activates rapid beclin1-dependent autophagy flux.

(A) Wildtype MEF expressing mRFP-EGFP-LC3B were exposed to full-nutrient control media (FM), amino acid (-AA) or glucose (-Glc) starvation, in the presence of Bafilomycin A1 (Baf A1) as indicated for 2 hrs. Starvation conditions contained 10% dialysed FBS. Autophagy membranes visible in the GFP and RFP channels are shown. Arrowheads show RFP(+) only (i.e. GFP-quenched, late) autophagosomes. Scale bar: 10 μm.

(B) GFP- and RFP- positive autophagy membranes were quantified in wildtype or ULK1/2 DKO MEF expressing mRFP-EGFP-LC3B following starvation conditions 1-6 for 2 or 18 hrs. Quantification using 30-40 cells from n=3 (2h experiment); or 20-32 cells from n=2 (18h experiment) (+/-SEM). P< (*) 0.05; (***) 0.001; by unpaired T-test, comparing conditions 3 vs. 4; 5 vs. 6.

(C) MEF (wildtype or with stable Beclin1 knockdown) were starved as indicated +Baf A1 for 2 hrs. Starvation conditions contained 10% dialysed FBS. Endogenous LC3B-positive autophagy membranes were detected and quantified in 120 cells (from n=2 experiments). Beclin1 knockdown efficiency was confirmed. (***) P<0.001; by ANOVA, Tukey's post-test.

Figure 3. Lack of autophagy flux following glucose starvation is conserved in cancer cells.

(A) The indicated cell types were incubated with glucose or amino acid starvation for 3 hours. As control, chloroquine (CQ, 25μM) was added to cells in full-nutrient conditions.

(B) MCF7 or A431 cells were treated to prolonged starvation (24hrs) as indicated. Starvation conditions contained 10% dialysed FBS. Cell lysates were analysed for LC3B, Sequestosome 1/p62 protein levels and S6 protein phosphorylation. Data representative of 3 experiments.

(C) MCF7 or A431 cells were starved as indicated for 3 or 24 hrs. Transcript levels for *LC3B* and *p62* were quantified (expressed as fold-change normalised to *GAPDH*; N=3 +/-SEM). Significant where indicated: P< (*) 0.05; (**) 0.01; (***) 0.001; (****) 0.0001; by ANOVA, Tukey's post-test.

(D,E) A431 cells stably expressing mCherry-EGFP-LC3B were starved as indicated +Baf A1 for 2 hrs. Starvation conditions contained 10% dialysed FBS. GFP- and RFP- positive autophagy membranes were quantified in 120 cells from n=3 experiments (+/-SEM). (****) P<0.0001 by unpaired T-test; comparing –AA vs. –Glc conditions. Scale bar: 10 μm.

Figure 4. Amino acid starvation triggers dephosphorylation of ULK1 serine 555 and autophagy.

(A) HEK293A cells were incubated under amino acid or glucose starvation conditions for 2 hrs. Where indicated, Bafilomycin A1 or 10% dialysed FBS were added. Immunoblotting detected LC3B lipidation, P-ACC and P-S6 levels in lysates.

(B) Quantification of LC3B lipidation ratios for n=3 experiments +/- SEM. (**) $P < 0.01$ unpaired T-test.

(C) HEK293A cells were starved of amino acid or glucose for the indicated times. All conditions contained Bafilomycin A1. Quantification for n=3 experiments +/- SEM. P< (*) 0.05; (**) 0.01; by ANOVA, Tukey's post-test, comparing UT to –AA conditions.

(D) HEK293A cells were incubated under amino acid or glucose starvation for indicated times. Starvation conditions contained 10% dialysed FBS. Parallel wells of control cells were replenished with full nutrient media at the start of incubation. Cell lysates were analysed for ULK1 serine 555 phosphorylation, P-ACC, LC3B and p62 levels. Representative quantification shown below phospho-blots. Quantification of p62 degradation and LC3B ratios for n=3 experiments +/- SEM. (***) $P < 0.001$ by ANOVA, Tukey's post-test.

(E) HEK293A stably expressing mCherry-EGFP-LC3B were incubated in the indicated starvation conditions (1-6) for 2 hrs. Starvation conditions contained 0.1% dialysed FBS. P< (**) 0.01; (****) 0.0001; by unpaired T-test, comparing conditions 3 vs. 4; 5 vs. 6. Scale bar: 10 µm.

Figure 5. Glucose starvation inhibits autophagosome formation.

(A) HEK293A cells were incubated under amino acid or glucose starvation for 2 hours. Starvation conditions contained 0.1% dialysed FBS. Cells were stained for endogenous ULK1- or p62-labelled autophagosomes. Scale bar: 10 µm.

(B) HEK293A cells were starved as in (A) for times indicated. Quantification of ULK1 and p62 puncta/cell. Each box represents n=38 cells, representative of 2 experiments.

(C) Wildtype MEF expressing GFP-DFCP1 were starved of amino acids as in (A) for 2 hours. Cells were stained for endogenous p62 puncta. Arrow points to autophagosome shown in zoom. Scale bar: 10 µm.

(D) HEK293A cells were starved of amino acids for 2 hours. Starvation conditions contained 0.1 or 5% dialysed FBS; or addition of MRT68921 (10µM) as indicated. Each box represents n=40 cells, representative of 2 experiments. (****) P<0.0001 by ANOVA, Tukey's post-test.

(E) HEK293A cells were starved of amino acids, glucose, or both together, for 2 hours. Dialysed serum concentrations were also varied during starvation as indicated. Each box represents n=40-50 cells, representative of 2 experiments. (****) P<0.0001 by ANOVA, Tukey's post-test.

814 **Figure 6. Differential effects of glucose and amino acids (glutamine, leucine and**
815 **arginine) on autophagy signalling.**

816 **(A)** HEK293A cells were starved of amino acids, glucose, or both together, for 2 hours.
817 Starvation conditions contained 10% dialysed FBS. Bafilomycin A1 was included as
818 indicated. Cell lysates were analysed for LC3B lipidation and quantified from n=3
819 experiments +/- SEM. (*) P<0.05 by unpaired T-test.

820 **(B)** HEK293A cells were starved as in (A) and analysed for P-ACC, P-S6 and
821 phosphorylation at the indicated ULK1 sites. Representative quantification shown below
822 phospho-blots.

823 **(C)** HEK293A cells were starved of amino acids (in the presence of 10% dialysed FBS).
824 Where indicated, starvation media contained Bafilomycin A1; and addback of amino acids
825 glutamine (Q), leucine (L) or arginine (R). Data representative of n=3 experiments.

826 **(D,E)** HeLa cells were starved of amino acids (in the presence of 5% dialysed FBS) with
827 addback of amino acids as indicated. Endogenous p62 puncta were analysed. Scale bar: 10
828 µm. (D) Each plot represents n=40 cells, representative of 2 experiments. (****) P<0.0001 by
829 unpaired T-test.

830

831

832 **Figure 7. Glutamine, leucine and arginine activate MTORC1 and inhibit ULK1 complex**
833 **translocation to autophagosome assembly sites.**

834 HEK293A cells stably expressing LAMP1-mRFP were starved of amino acids (for 2 hrs), or
835 starved for 110 min followed by 10 min re-supplementation of glutamine, leucine and
836 arginine (in the presence of 5% dialysed FBS). Fixed cells were stained for endogenous (A)
837 MTOR, (B) ULK1, or (C) ATG13. Arrows in zoomed insets show: (A) MTOR localised on
838 lysosomal membranes in response to glutamine, leucine and arginine; (B) and (C),
839 localisation of the ULK1 complex on autophagosome assembly sites juxtaposed to
840 lysosomal membranes in response to amino acid starvation. Scale bars: 10 µm.

841

Figure 8. Inhibition of autophagosome formation by AMPK.

(A) HEK293A cells were starved of amino acids in the presence or absence of A769662 (50 µM) for 2 hours. Starvation conditions contained 5% dialysed FBS. Cell lysates were analysed for phosphorylation of ACC and S6.

(B) HEK293A stably expressing mCherry-EGFP-LC3B were incubated in starvation conditions (1-5) for 2 hrs. Starvation conditions contained 0.1% dialysed FBS. Scale bar: 10 µm.

(C) Quantification of (B). Each plot represents 135 cells +/- SEM from n=3 experiments. **** P<0.0001 by unpaired T test; comparing conditions 2 vs 3, and 4 vs 5 (for both GFP and RFP quantifications).

(D) HEK/ mCherry-EGFP-LC3B cells as in (B) were starved of amino acids, or amino acid and glucose together, for 2 hours. Starvation conditions contained 0.1% dialysed FBS. Each plot represents 45 cells +/- SEM, representative of 3 experiments. **** P<0.0001 by unpaired T test; comparing –AA vs double starved conditions (for both GFP and RFP quantifications).

Figure 9. Phosphorylation of ULK1 by AMPK inhibits autophagosome formation.

(A) HEK293A cells were starved of amino acids in the presence or absence of A769662 (50 μM) for 2 hours. Starvation conditions contained 0.1% dialysed FBS. Fixed cells were stained for endogenous p62- or ULK1- autophagosomes and quantified. Each plot represents 135 cells from n=3 experiments. **** P<0.0001 by unpaired T test.

(B) ULK1/2 DKO cells were reconstituted with Myc-ULK1: wildtype or 4SA (S467A, S555A, T574A, S637A). Expression levels were confirmed by immunoblotting with anti-ULK1 antibody.

(C) ULK1/2 DKO cells reconstituted with wildtype or 4SA Myc-ULK1 were starved of amino acids in the presence or absence of A769662 for 2 hours. Starvation conditions contained 10% dialysed FBS. Fixed cells were stained for endogenous p62 puncta. Scale bar: 10 μm.

(D) Experiment in (C) was quantified. Each plot represents 90-135 cells from n=3 experiments. (***) P < 0.001 by ANOVA, Tukey's post-test.

(E) Cells as in (C) were starved of amino acids, or amino acid and glucose together, for 2 hours. Starvation conditions contained 10% dialysed FBS. Each plot represents 135 cells from n=3 experiments. (***) P < 0.001 by ANOVA, Tukey's post-test.

Figure 10. Glucose starvation and AMPK inhibit lysosomal acidification.

(A,B) HEK293A cells were starved of amino acids for 2 hours and stained using Lysotracker red DND-99. Starvation contained 0.1% dialysed FBS. Where indicated, starvation included CQ or Bafilomycin A1. Lysotracker staining intensity per cell was quantified from confocal images (arbitrary units). Each box represents n=60 cells, representative of 4 experiments.

(C) HeLa cells were starved of serum, amino acids or glucose for 2 hours and analysed for lysotracker staining. Amino acid and glucose starvation conditions contained 0.1% dialysed FBS.

(D) Quantification of (C). Each box represents n=50-60 cells, representative of 4 experiments.

(E) Experiment in (C,D) repeated in HEK293A cells. Each box represents n=50-60 cells, representative of 4 experiments.

(F,G) Wildtype or ATG5 knockout MEF were starved and analysed as in (C). Each box represents n=40-50 cells, representative of 5 experiments.

(H) ULK1/2 DKO or FIP200 KO MEF were starved of amino acids and analysed as in (C,D). Each box represents n=270-320 cells from 3 experiments.

(I) HEK293A cells were starved of amino acids, or amino acid and glucose together, for 2 hours as in (C). Where indicated, the double-starvation condition contained addback of D-glucose (1 g/L). Each box represents n=60 cells, representative of 4 experiments.

(J,K) Wildtype MEF (or HEK293A **(L)**) were starved of amino acids in the presence or absence of A769662 (50 µM) for 2 hours and analysed as in (C,D). Each box represents n=120 cells from 2 experiments. **** P<0.0001 by unpaired T test. Scale bars: 20 µm.

MCB

Molecular and Cellular Biology

Molecular and Cellular Biology

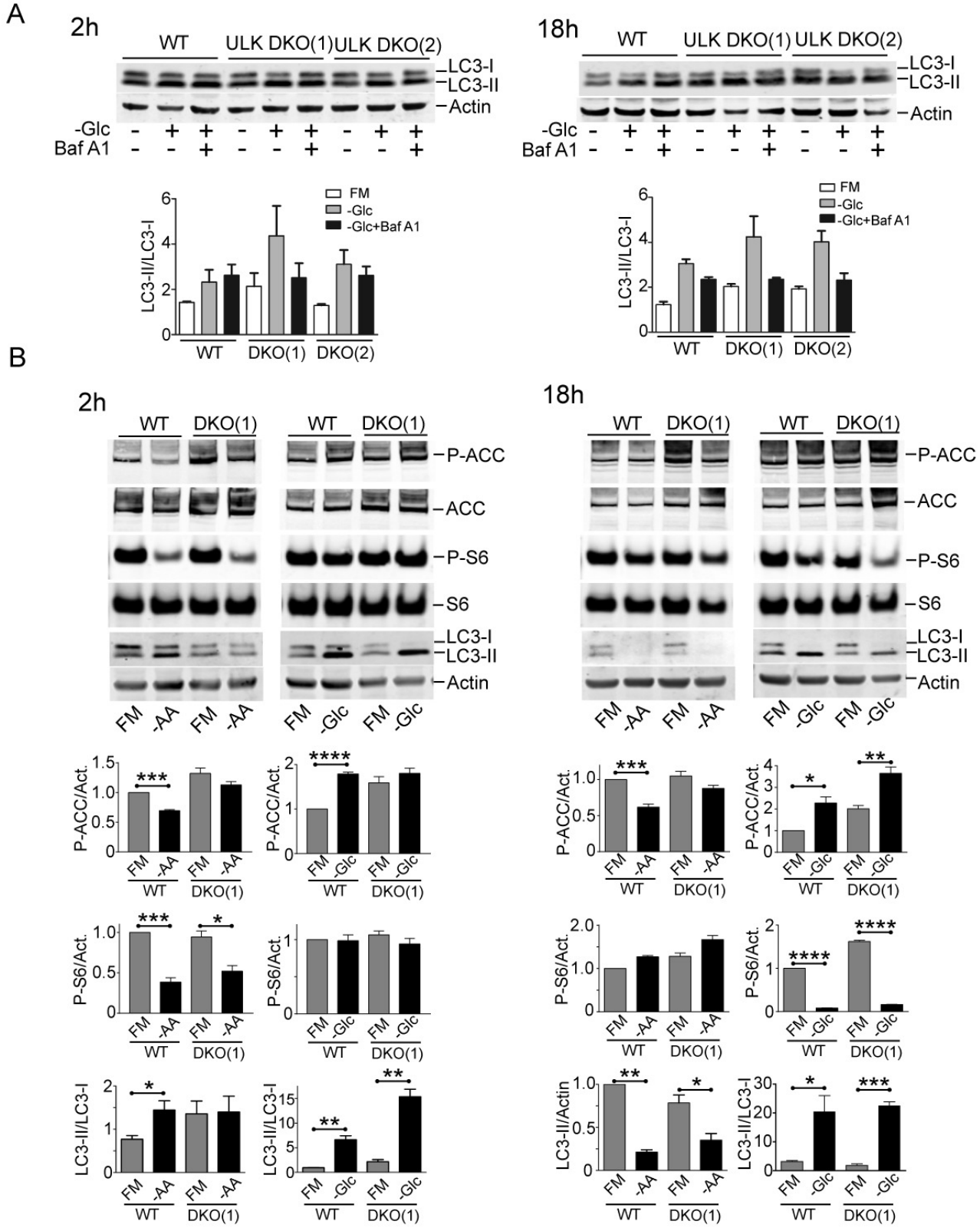

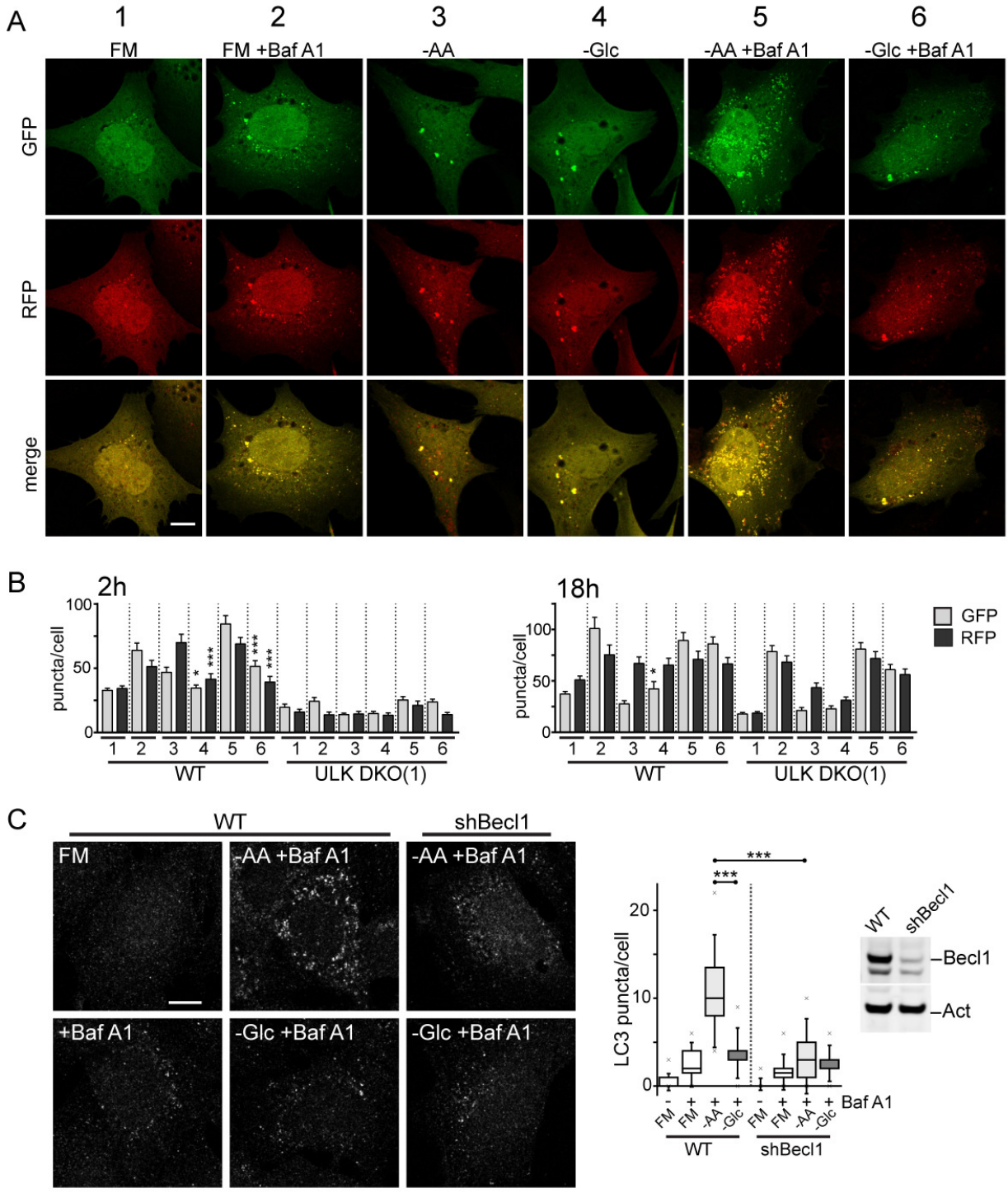

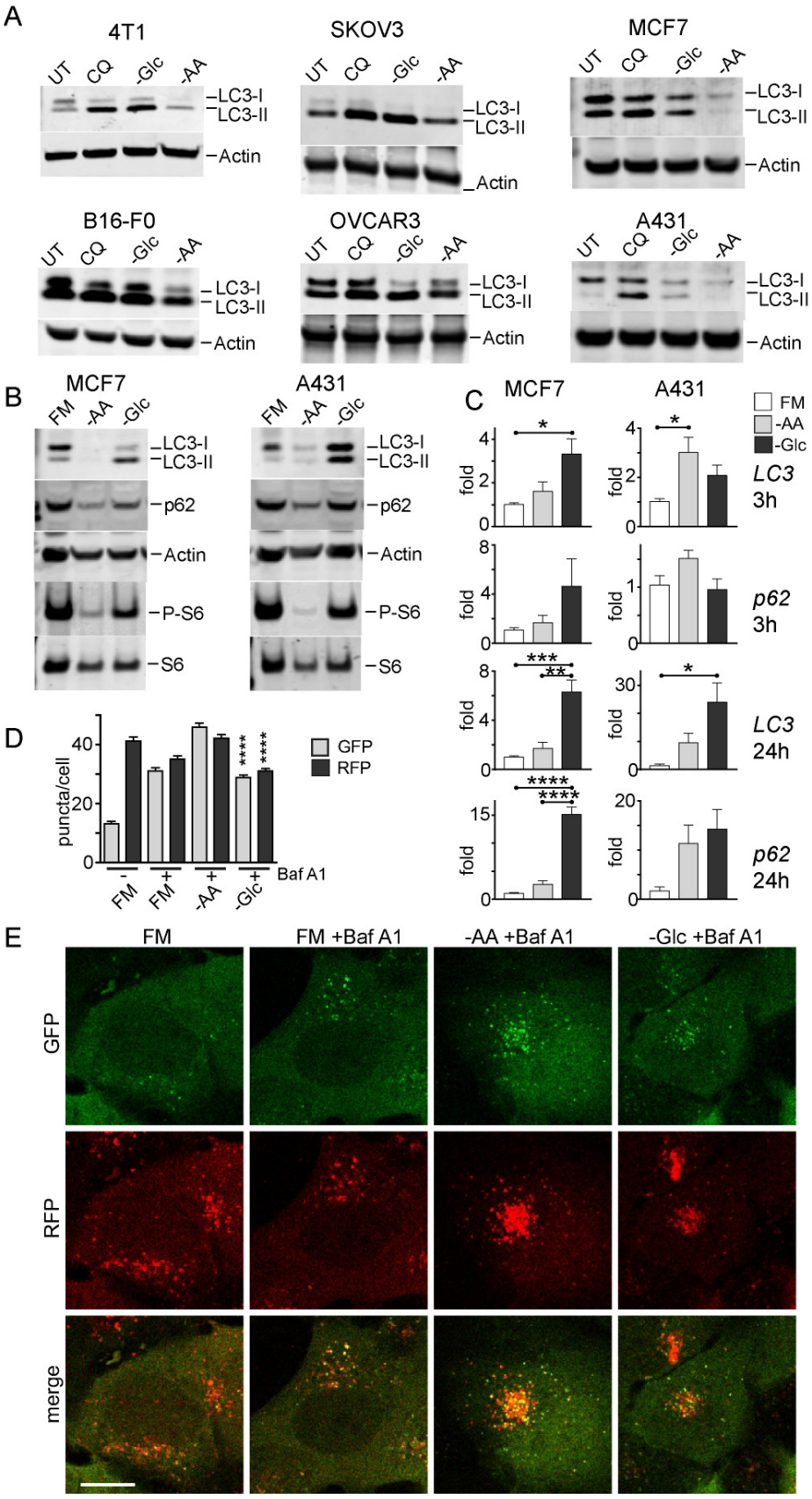

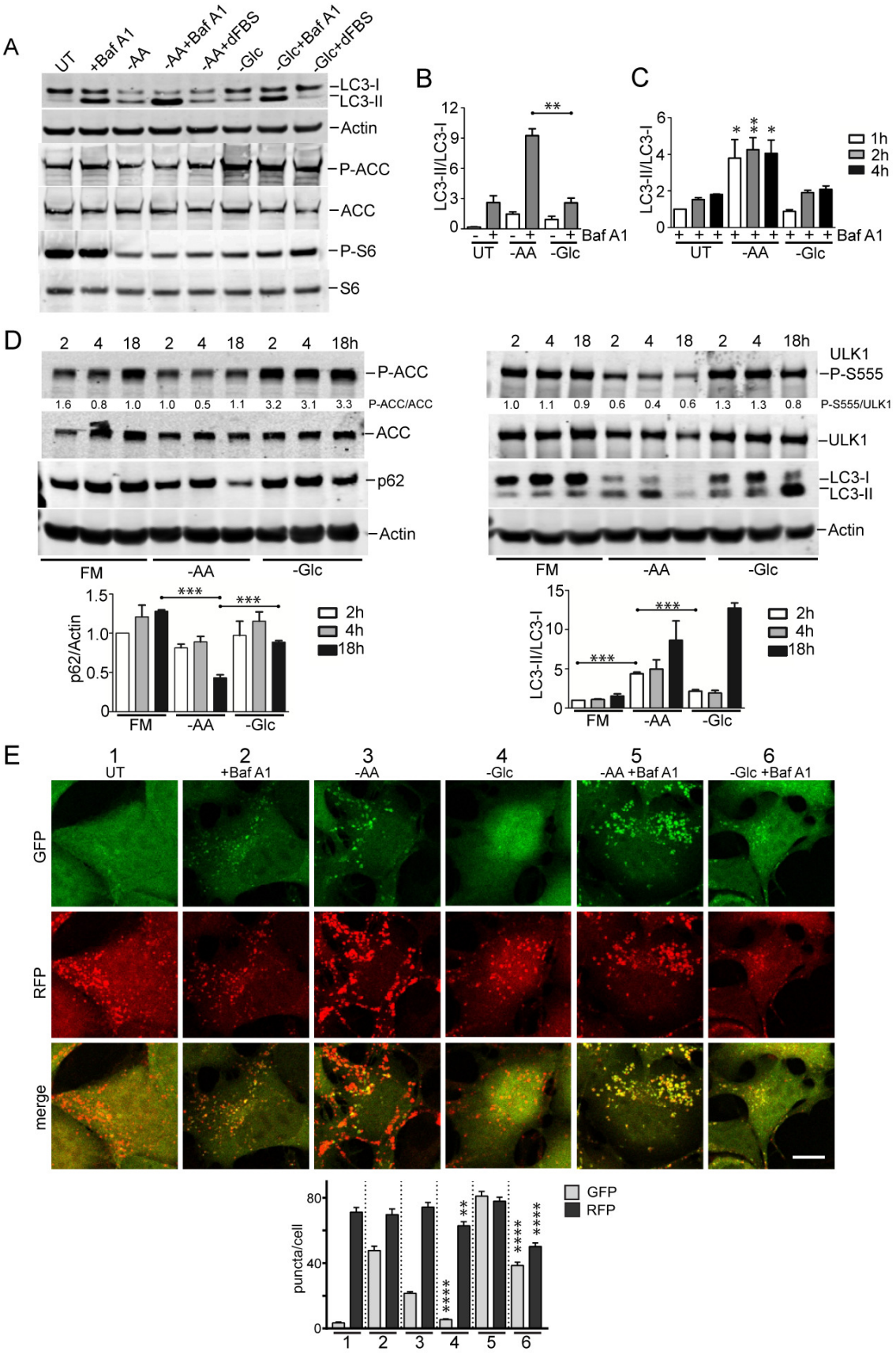

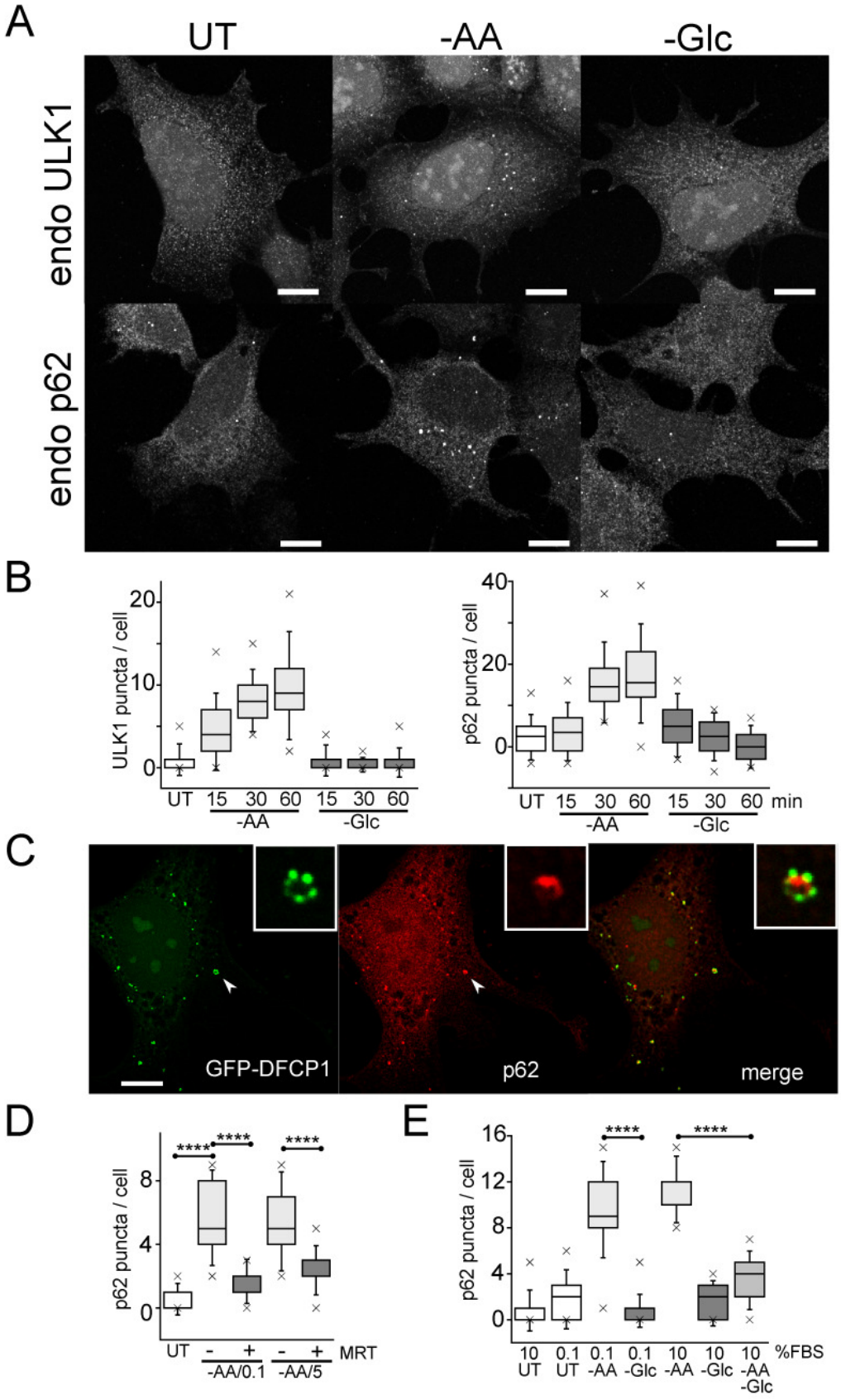

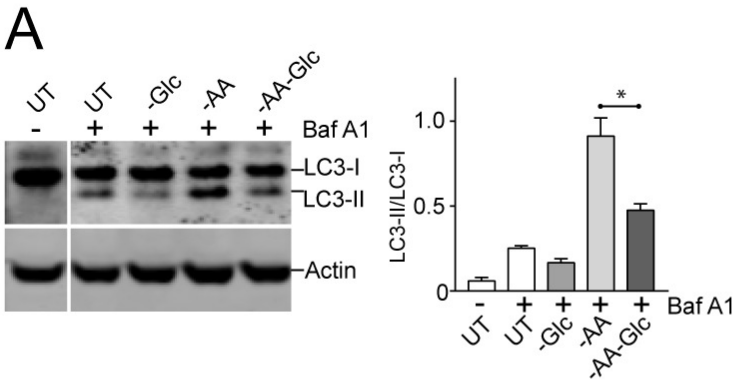

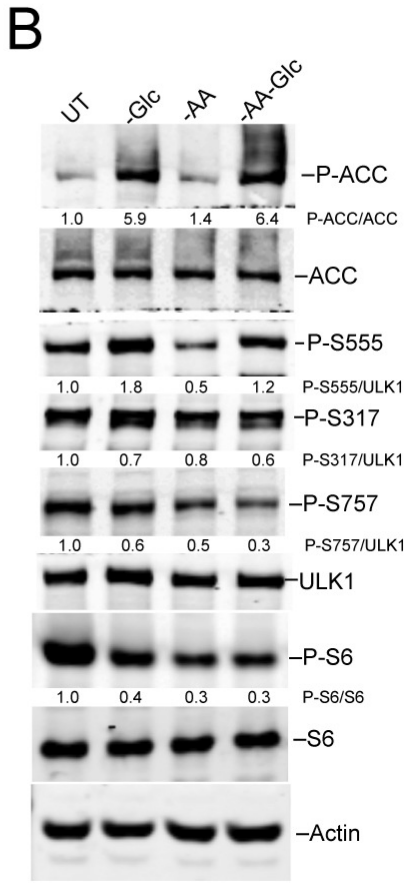

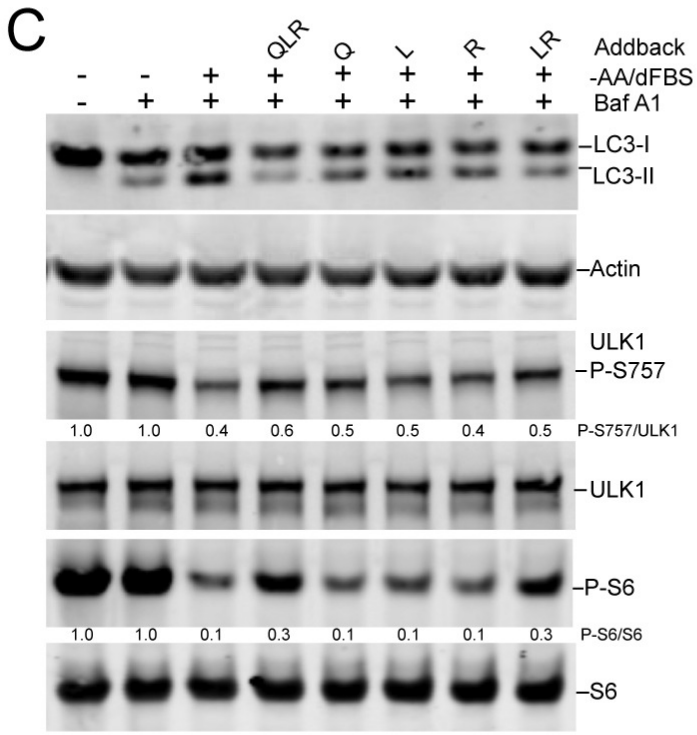

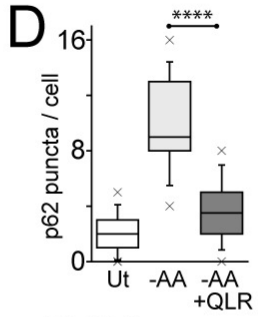

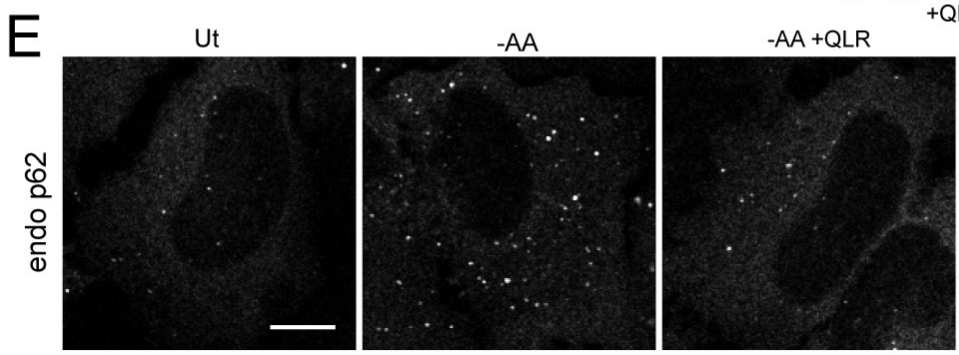

Molecular and Cellular Biology

Molecular and Cellular Biology

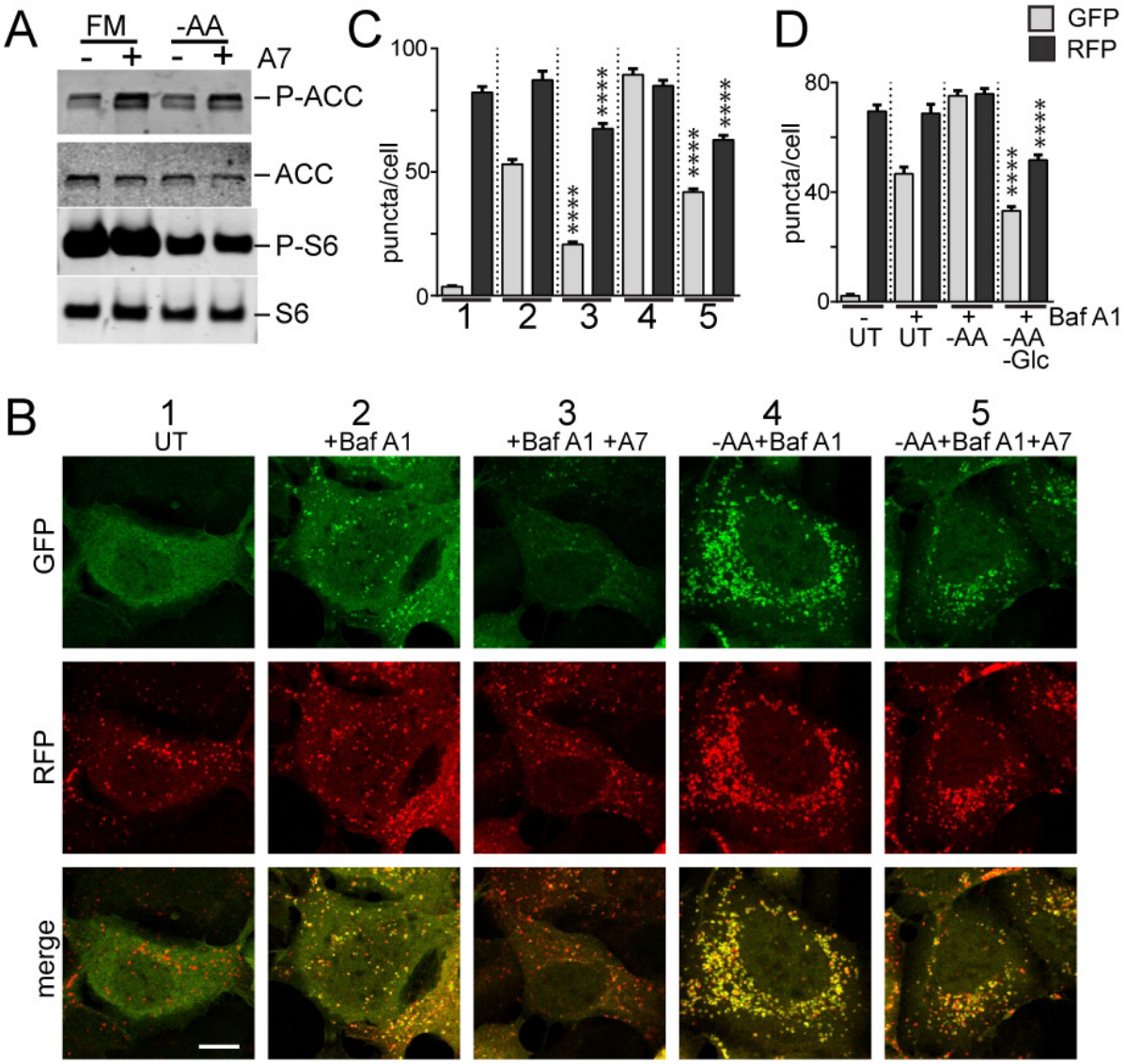

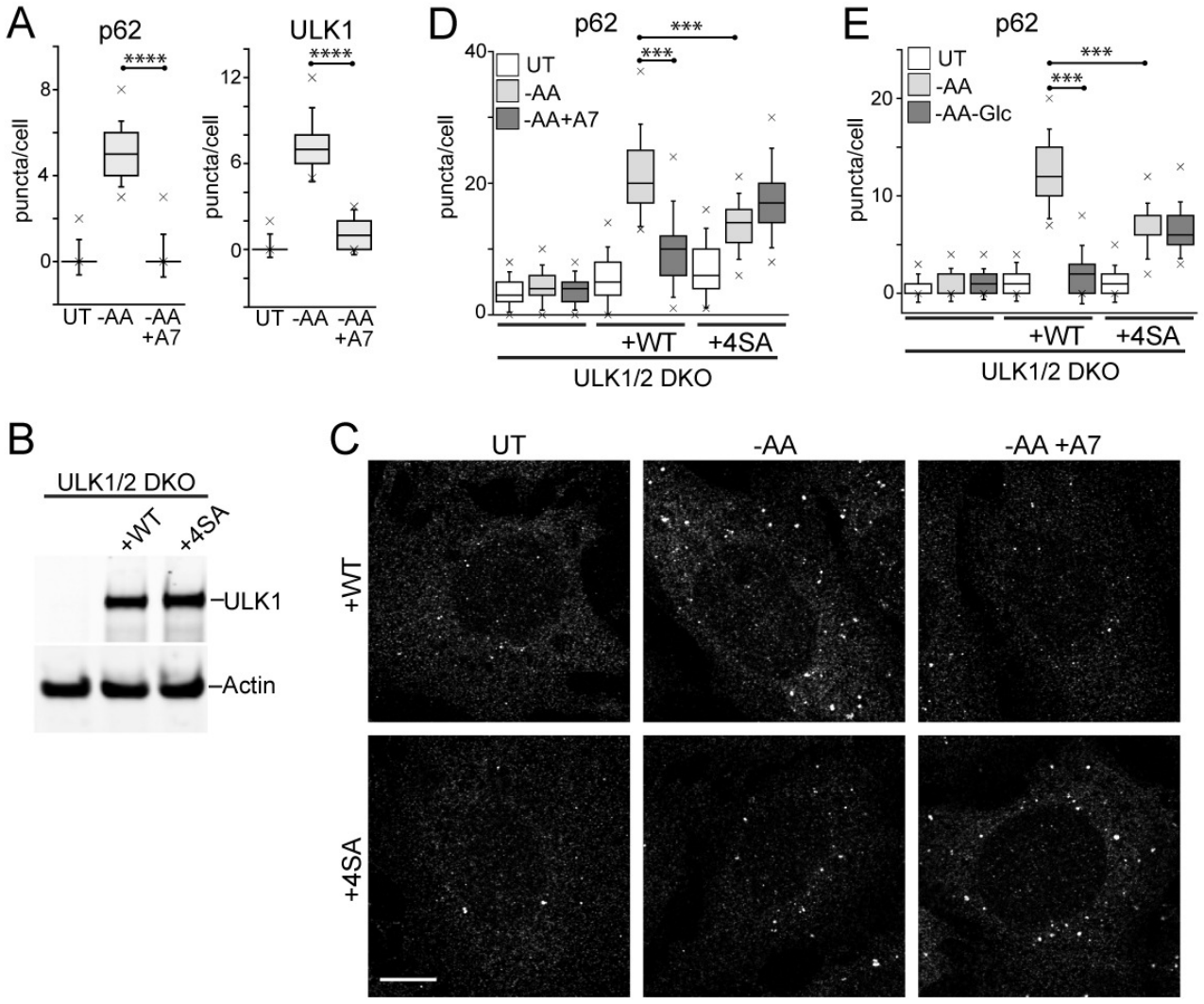

Molecular and Cellular Biology